Acidity and Salt Precipitation on the Vasa; The Sulfur Problem

Proceedings
8th ICOM-CC WOAM Conference
Stockholm 11-15 June 2001

Magnus Sandström,[a] Farideh Jalilehvand,[b] Ingmar Persson,[c] Ulrik Gelius[d]
and Patrick Frank.[b]

[a]Department of Structural Chemistry, University of Stockholm, SE-106 91 Stockholm, Sweden

[b] SSRL, Stanford Linear Accelerator Center, P.O. Box 4349, MS 69, Stanford, CA 94309, USA.

[c]Department of Chemistry, Swedish University of Agricultural Sciences, P. O. Box 7015, SE-750 07 Uppsala, Sweden

[d]Department of Physics I, Ångström Laboratory, Uppsala University, P.O. Box 530, SE-75121 Uppsala, Sweden

Acidity and Salt Precipitation on the Vasa; The Sulfur Problem

Abstract

The present major conservation problem for the Vasa is the oxidation of sulfur compounds in the wood, which after several intermediate steps results in sulfuric acid and high acidity leading to wood degradation. In February 2001 the extent of this problem was disclosed by analyzing two core samples of oak wood from a massive oak beam in the hold at the bottom of the ship, down to 80 mm depth. Electron spectroscopy for chemical analysis (ESCA or XPS) was used for quantitative measuements of all elements present in significant amounts in one core sample, and in the other the different forms of sulfur were analyzed by means of synchrotron based sulfur K-edge X-ray absorption spectroscopy (XANES). Both the ESCA and the XANES results show the total sulfur concentration to be highest at the surface, with sulfate as the dominating form, SO_4^{2-}. The relative amount of non-oxidized sulfur, mainly elemental sulfur, increases rapidly below the surface, but the total sulfur concentration decreases at the same time. Deep below the surface at low sulfur concentration again oxidized sulfur, mostly sulfate, dominates. The XANES spectra clearly show several intermediate oxidation states of sulfur as minor components. Thus, below the surface to a depth of about 2 cm reduced sulfur, mainly elemental sulfur, is present in significant amount, about 0.5 mass%. If the sulfur concentration in this core is representative, as also later analyzes indicate, the corresponding amount of concentrated sulfuric acid may when all sulfur is oxidized be about 0.5 kg/m^2 wooden surface, or totally more than 5000 kg for the Vasa!

The ESCA analyses show a rather high and only slowly decreasing level of oxidized borate at all depths. Since borate is not naturally present in oak wood, this shows that boric acid from the solutions used in the initial conservation treatment, has penetrated deep into the wood. Iron is present in oxidized form with rapidly decreasing concentration below the surface, as also for chloride and calcium. Silicon was only found in the surface layer, while sodium occurred with constant concentration at all depths.

Surface salt precipitations sampled inside the hull of the Vasa were analyzed by means of X-ray powder diffraction (XRD) and sulfur K-edge XANES spectroscopy. The XRD analyzes showed that the crystalline part of the samples contained sodium, ammonium, potassium, calcium and magnesium sulfates of various composition; in most cases gypsum $CaSO_4 \cdot 2H_2O$, but also lecontite (K, NH_4)$NaSO_4 \cdot 2H_2O$, mascagnite $(NH_4)_2SO_4 \cdot 2H_2O$ and starkeyite $MgSO_4 \cdot 4H_2O$. Iron sulfates, especially natrojarosite $NaFe_3(SO_4)_2(OH)_6$ but also melanterite $FeSO_4 \cdot 7H_2O$, were found and in a some places crystals of elemental α-sulfur (brimstone S_8) but only traces of pyrite, FeS_2. The XANES spectra showed in the surface samples in addition to the dominating sulfates, also some amount of elemental sulfur.

The salt formation on the surface is a sign of an ongoing production of sulfuric acid, which will cause high acidity and wood degradation. The high concentration of sulfur compounds found in the wood shows that this is a severe threat to the Vasa. Lowering the relative humidity RH noticeably will only marginally slow down the reaction rate of a chemically controlled oxidation process, and gives unfavorable side effects. The presence of iron in the wood, and corroding iron bolts, gives additional problems because of the catalytic effect of iron on the oxidation process. It seems important to keep the conditions constant, the RH but also the temperature, in order to prevent water and oxygen migration in the wood, and to apply pH raising and iron removing consolidation treatments to the already acidified wood. Possible treatments are proposed.

Introduction

After the rainy summer in the year 2000, salt formation and high acidity was observed in many places on the surfaces inside the Vasa's hull, as well as upon individual objects held in the stores and displayed in the ship hall of the Vasa Museum. To acquire knowledge about the physical phenomena involved and to find suitable treatments, a seminar was held 12-13th of February 2001 in the Vasa museum, and analyzes were started. From previous experience of similar conservation problems [1,2], this salt formation was suggested to be an effect of the impregnation of sulfides into the oak wood during its immersion for 333 years at about 32 m depth into the water in the Stockholm harbor. The presence of corroding iron in anaeorobic conditions could possibly give rise to the formation of pyrite in the wood, as had been observed in other cases [1,2]. The oxidation processes of sulfides and iron can in different ways damage the wood. One is the mechanical damage because of the volume expansion when sulfides/sulfur are oxidized to sulfates, *cf.* Table 1. The other aspect, and evidently a more serious problem, is the production of sulfuric acid (hydrolyzed to $2H^+ + SO_4^{2-}$ for pH > 2), which occurs at the oxidation of sulfur, e.g. according to the overall redox reactions:

$$H_2S + Fe_2(SO_4)_3 \rightarrow 2\ FeSO_4 + H_2SO_4 + S(s) \tag{1}$$
$$S(s) + {}^3/_2\ O_2 + H_2O \rightarrow H_2SO_4 \tag{2}$$
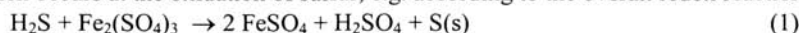
The resulting acidity (values down to pH=2 occur in many places) is known to damage the wood by acid hydrolysis, and also iron(III) ions are known to catalyze the degradation of cellulose [1]. The salt precipitation seemed to be connected to the variations in the relative humidity, which at several occasions deviated from the preset level of about 60%, reaching values more than 65% during the year 2000.

Another factor to consider is the conservation treatment of the VASA, the first major object to be impregnated with polyethylene glycol (PEG) solutions [3]. In the initial stage (the spraying lasted 17 years) also borates/boric acid were used in the fluid, to prevent microbial activity. PEG is a water soluble polymer linked via ether oxygens and with terminal hydroxo groups, $H(OCH_2CH_2)_nOH$. The PEG used had the lowest molecular weight of 600, and the highest that was used for surface treatment about 4000, thus with the number of units (n-values) between about 12 and 90. Many of the more than 8000 iron bolts, replacing the old ones in Vasa, are now corroding in the PEG treated wood. Also, there are indications that PEG interacts with iron ions and degrades with time.

Table 1. Expansion of sulfides when oxidized to sulfate.[a]

Mineral	Formula	Volume per S-atom/$Å^3$	Volume factor
Pyrite	FeS_2	20	1
Mackianawite	$Fe_{1-x}S$	34	1.7
α-Sulfur	S_8	51.5	2.6
Rozenite	$FeSO_4 \cdot 4H_2O$	163	8.2
Melanterite	$FeSO_4 \cdot 7H_2O$	244	12.2
Jarosite	$NaFe_3(SO_4)_2(OH)_6$	399	20
Gypsum	$CaSO_4 \cdot 2H_2O$	494	25

[a] Volumes taken per formula unit in crystal structure of mineral

For the future preservation of Vasa it is essential to find solutions to these combined problems. Samples were taken and analyzed starting February 2001, and the present report summarizes the results of the analyses and studies made so far. The strategy was to determine the corrosion products on the surface by means of X-ray powder diffraction (XRD), a method capable of identifying the main crystalline compounds. The degree of penetration into the wood was obtained from analyzing the amount and gradient of the elements down to 80 mm depth in a core sample by means of X-ray photoelectron spectroscopy (XPS, also called ESCA, electron spectroscopy for chemical analyses). For some elements the chemical shifts of the electron binding energies from ESCA can give useful information about the oxidation state and chemical surrounding of an element in the sample. However, the method is very sensitive to surface contamination, all the signal comes from a surface layer $< \sim100$ Å, and the high vacuum needed in the spectrometer may lead to surface alteration and loss of volatile substances, especially water from hydrated samples. Moreover, the resolution is limited for the sulfur analyses. We therefore also used synchrotron based X-ray absorption spectroscopy (XAS), or more precisely sulfur K-edge X-ray absorption near-edge spectroscopy (XANES), which gives good resolution high sensitivity for sulfur in different chemical states. XANES is not as surface sensitive and can be used for samples at atmospheric pressure in helium atmosphere, but is more difficult to use for quantitative analysis. To our knowledge these two techniques, ESCA and XANES, have not been applied on this type of problem before. Elemental sulfur analysis was also performed to establish the total sulfur concentration in various sections of the core.

Experimental

Samples. A set of samples were taken from a number of salt-covered surfaces inside the hull of Vasa (see Table 2 and Figure 1), and analyzed by X-ray powder Diffraction (XRD). Also, two cores, 70 and 84 mm, were taken by drilling into an oak beam close to the bottom of the ship (W8). One core was analyzed by means of ESCA for a number of elements at various depths (Table 3). From the other core, samples were taken at various depths, 1, 2, 7, 14, 21 and 66 mm below the surface, and were analyzed for different oxidation states of sulfur by means of sulfur K-edge XANES at the synchrotron in Stanford Synchrotron Radiation Laboratory, SSRL. In addition, the surface samples S3, S4, S7, S8 (*cf.* Table 2), pyrite powder and some other standards were measured by sulfur K-edge XANES (Table 4).
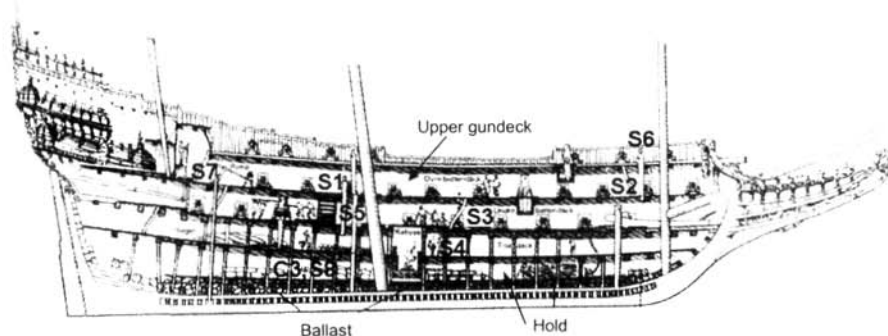

Figure 1. An outline of the hull of Vasa with sample positions indicated. C3 for core, S1-S8 for surface XRD samples. Dimensions: length 61 m (69 m including bowsprit), max. width 11.7 m, stern castle 19.3 m high, total surface area 14 000 m².

XRD measurements. A Guinier-Hägg camera was used with Cu $K\alpha_1$ X-ray radiation, 1.5406 Å (in a few cases Cr $K\alpha_1$, 2.2897 Å, was used to reduce fluorescence from iron in the samples). By means of a specially constructed scanner, the film data were digitalized and the background eliminated. This method is suitable for small amounts of sample, and to obtain high resolution with good precision. No internal calibration compound (such as pure silicon Si) is necessary, which would further complicate the already line-rich spectra. Spectra were obtained in the 2θ range 10 to 87 degrees. Crystalline components were identified by means of the Powder Diffraction File (PDF) data base, with the PDF number given in Table 2.

ESCA measurements. Thin slices (about 0.3 to 1 mm) with about 5 mm diameter were taken at various depths of the oak-core (*cf.* Table 3), and mounted on tape in the sample chamber of a Scienta ESCA 300 instrument [4]. This powerful and sensitive type of ESCA instrument allows sulfur analyses of fair accuracy. More than 1 hour pumping was required to reduce the vapor pressure (mainly water) from the samples down to levels for which measurements were possible. The pressure was 10^{-8} mbar when starting the measurements, and often at $4 \cdot 10^{-9}$ mbar at the end of the analyses. High intensity monochromatic Al K_α X-ray radiation (1487 eV) was used to excite photoelectrons from the core shells of all elements in the samples, Figure 2. For sulfur 2p electrons were analyzed. A sample area of approximately 5x2 mm was irradiated and a mask of aluminium foil was used to prevent contributions from the sample holder. The following elements were found to occur in significant amounts in different samples of the oak rod: B, C, N, O, S, Si, Cl, Fe, Na, Ca. The elements Li, K, P and Mn, were below the detection limit.
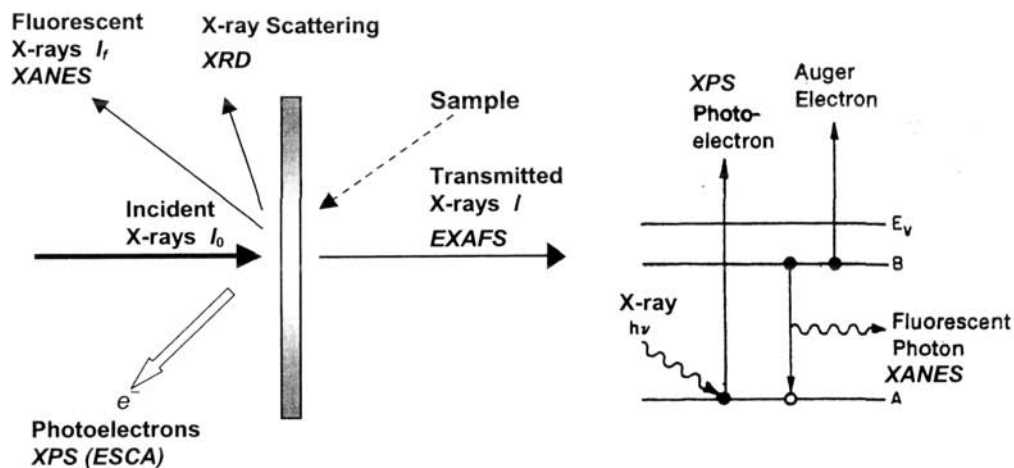

Figure 2. (left) X-rays absorbed in a sample generate photoelectrons (XPS spectra), followed by fluorescence (XANES, EXAFS) and Auger-electrons. Diffracted X-rays are used for XRD, and transmitted for EXAFS spectra; (right) When the hole after an excited core electron is filled fluorescent photons and Auger electrons are ejected.
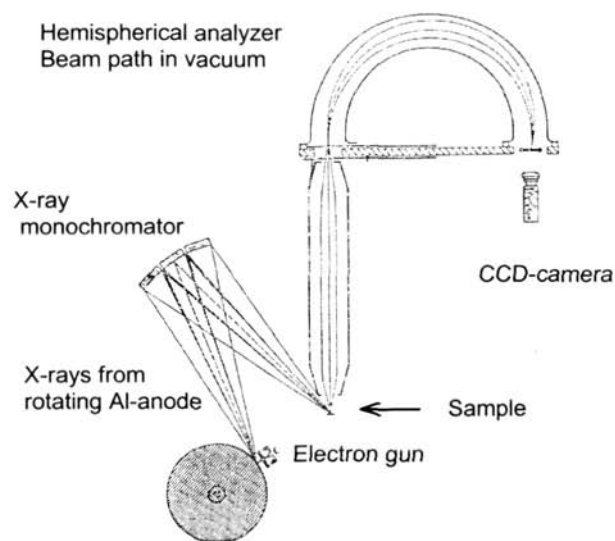
Hemispherical analyzer
Beam path in vacuum

X-ray
monochromator

CCD-camera

X-rays from
rotating Al-anode

Sample

Electron gun

Figure 3. Principle of the ESCA 300 spectrometer [4]. Photoelectrons generated by high intensity monochromatic Al K_α X-rays (1486.7 eV) are focused in high vacuum by means of an electrostatic field on a multichannel detector, giving a precise value of the binding energy of the core electrons in the elements of the different compounds in the surface layer of the sample (<100 Å).

XANES measurements. Sulfur K-edge X-ray absorption spectra were collected on beamline 6-2 at the Stanford Synchrotron Radiation Laboratory (SSRL) under dedicated conditions. The SPEAR synchrotron of SSRL operates at 3.0 GeV and a maximum current of 100 mA. The energy of the very intense X-rays from the wiggler beam line was varied using a Si(111) double-crystal monochromator and a nickel-coated mirror to reject higher order harmonics of the X-rays passing through the monochromator, *cf.* Figure 4 [5]. The X-ray intensity incident on the sample was monitored using a helium-filled ion chamber I_0. All the beam-path is through helium, and the sample was held in helium at atmospheric pressure. The X-ray fluorescence, which occurs after the emission of a photoelectron (*cf.* Figure 2), is proportional to the absorption of X-rays in the sample. The fluorescence was measured by means of a Stern-Heald-Lytle fluorescent ion chamber detector without filter or Soller slit, Figure 4. The energy scale was calibrated before every measurement against the lowest energy peak of a sodium thiosulfate standard, which was set to 2472.0 eV at the peak position. The energy resolution of the spectra is estimated to be about 0.5 eV, and the precision of the relative peak positions within ± 0.1 eV. All data were collected at room temperature. The samples were finely ground and a thin layer spread out on a sulfur-free mylar tape, except for the oak-wood core rod for which thin slices, about 8-10 mg, were hacked into small pieces by means of a razor blade, or pulverized by means of a file in inert atmosphere.
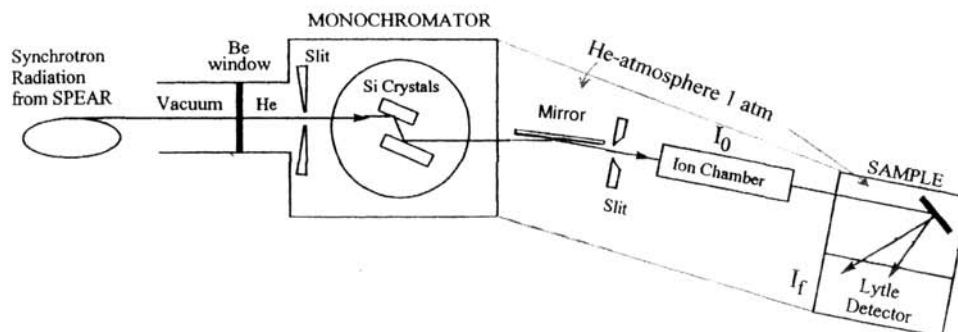
Figure 4. Sulfur K-edge X-ray absorption measurements on the SSRL beamline 6-2 using synchrotron X-ray radiation from SPEAR. Characteristics: Sample in atmospheric pressure (He), rejection of harmonics by Ni-coated mirror, fluorescence detection (Lytle detector)

Results

I. XRD analyses. The main crystalline components were identified for all analyzed samples, Table 2. For all surface samples, except sample S2, the main crystalline component is a sulfate, the thermodynamically stable end product of sulfur oxidation. The borate found for S2 certainly comes from the plugs of borax, which were put into the empty holes for iron nails in an early stage of the conservation process, and later removed. For the sample S8, some glittering crystals were picked out from the surface scrapings around the site of the core samples and analyzed separately. The crystals were found to be elemental orthorhombic α-sulfur S_8, the mineral brimstone, which can form as an intermediate step under anaerobic conditions in the oxidation process of H_2S, see formula (1) above. Under reducing conditions, with redox potentials around zero, elemental sulfur can be the thermodynamically stable form [6], *cf.* the Pourbaix (E_H-pH) diagram in Figure 5, calculated for aqueous equilibrium conditions. If iron(III) ions are present in sufficient amount, then pyrite FeS_2 has a larger stability range for similar redox conditions, Figure 5. It is also known that elemental sulfur may form as a kinetic intermediate or as a metastable phase under many natural conditions, often in reactions catalyzed by bacteria [6,7]. Thus, the elemental sulfur stored in the wood of the Vasa has probably formed by transformation of the hydrogen sulfide penetrating into the wood during the time on the bottom in near anaerobic water. The encrustments enclosing the remaining timbers of the Batavia has evidently created an iron-rich anaerobic environment, consistent with the storage of sulfur predominatingly as pyrite in the wood, *cf.* Figure 5.

Samples S3, S4 and S8 were found to contain iron sulfates (melanterite $FeSO_4 \cdot 7H_2O$, natrojarosite $NaFe_3(SO_4)_2(OH)_6$), but only traces of pyrite, FeS_2, could be detected for the Vasa in core 3 down to a few mm below the surface of S8. The most commonly occurring sulfate in the samples is gypsum, $CaSO_4 \cdot 2H_2O$, which has low water solubility. The minerals can in some cases have variable composition, to some extent exchanging one ion for another in isostructural compounds, which gives very similar XRD patterns. For example, natrojarosite 36-0425 $NaFe_3(SO_4)_2(OH)_6$ can hardly be distinguished from 22-827 jarosite $KFe_3(SO_4)_2(OH)_6$ or hydronian jarosite 36-0427 (K,H_3O) $Fe_3(SO_4)_2(OH)_6$. Also lecontite has variable composition, *e.g.* 15-0370 $(K,NH_4)NaSO_4 \cdot 2H_2O$ and 15-0283 $NaNH_4SO_4 \cdot 2H_2O$, respectively. However, since the ESCA measurements showed no potassium in the samples, see below, the sodium salts should be dominating. Natrojarosite has higher stability than hydronian jarosite, and forms in a pH range between about 2 and 6 for reasonable concentrations of iron(III), sulfate and sodium ions if the precipitation of goetite FeOOH(s) is kinetically suppressed (Figure 5).

Table 2. Results of XRD analyses of surface samples from the Vasa[a]

Samples from the VASA Description	Major crystalline components PDF-number* Mineral name Formula
S1 White powder Upper gun-deck, behind pump	15-0370 Lecontite $(K, NH_4)NaSO_4 \cdot 2H_2O$
S2 Greyish powder, Foremast, around holes for iron bolt	24-1056 Sborgite $NaB_5O_8 \cdot 5H_2O$
S3 White crystals+yellow-brown powder; Lower gun-deck at staircase	22-0633 Melanterite $FeSO_4 \cdot 7H_2O$ 21-0816 Gypsum $CaSO_4 \cdot 2H_2O$ 36-0425 Jarosite $NaFe_3(SO_4)_2(OH)_6$ (minor)
S4 White cover on soft wood, Cooking place, end of oak-beam	21-0816 Gypsum $CaSO_4 \cdot 2H_2O$ 36-0425 Jarosite $NaFe_3(SO_4)_2(OH)_6$
S5 Yellow-grey powder Stern-mast, around hole for iron bolt	10-0343 Mascagnite $(NH_4)_2SO_4 \cdot 2H_2O$ + unknown (minor)
S6 Grey-white powder Ornamental head, star-board by foremast	15-0370 Lecontite $(K, NH_4)NaSO_4 \cdot 2H_2O$ 21-0816 Gypsum $CaSO_4 \cdot 2H_2O$ (minor)
S7 White powder on soft wood (linden tree) Head of lion on gun-port, Item 216 in magazine	24-0720 Starkeyite $MgSO_4 \cdot 4H_2O$ or 15-0370 Lecontite $(K,NH_4)NaSO_4 \cdot 2H_2O$ (minor) 21-0816 Gypsum $CaSO_4 \cdot 2H_2O$ (trace)
S8 Brown-black surface layer on oak beam in the hold close to drill holes for core samples	36-0425 Jarosite $NaFe_3(SO_4)_2(OH)_6$ 21-0816 Gypsum $CaSO_4 \cdot 2H_2O$ 8-0247 α-Sulfur S_8 (brimstone, minor)

Calibration Samples:

WPYR2 Freshly ground pyrite powder with metallic luster.	01-1295 Pyrite FeS_2, sharp lines from a well-crystallized sample
WPYR1 Grey pyrite powder (particle size < 32 μm) stored for 10 years.	01-1295 Pyrite FeS_2, 25-0421 Rhomboclase $HFe(SO_4)_2 \cdot 4H_2O$.
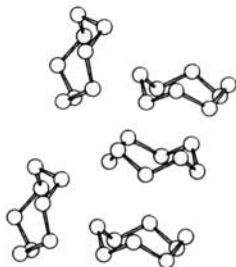
Elemental sulfur with S_8 rings
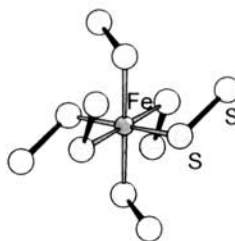
Pyrite FeS_2 with disulfide ions S_2^{2-}

[a] Powder Diffraction File Number (PCPDFWIN version 1.30)

74

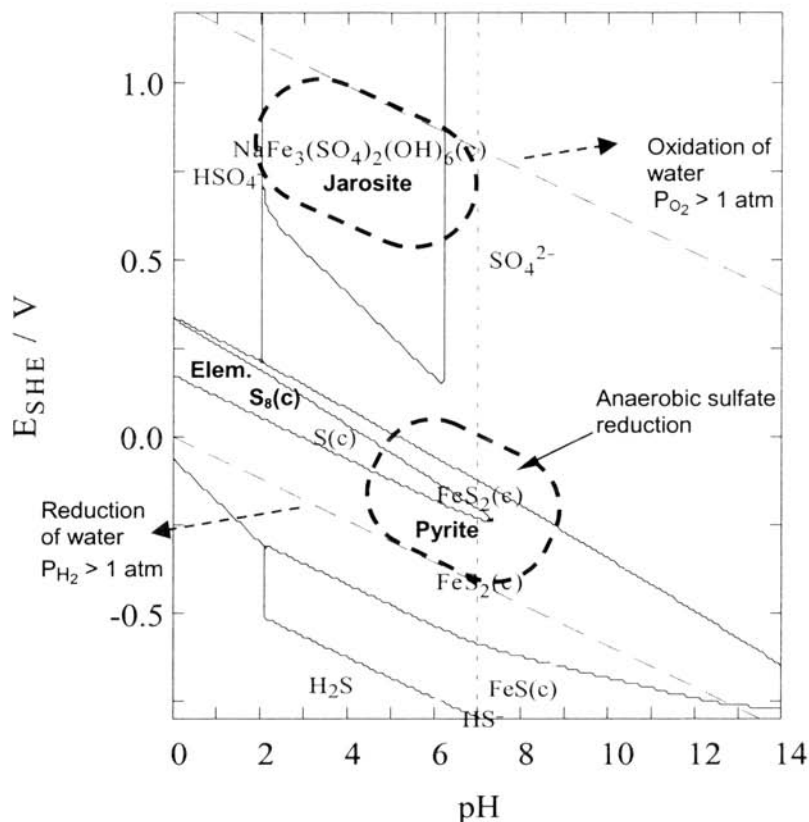*Figure 5. Predominant sulfur species in equilibrium with iron and sodium ions in aqueous solution (calculated for $[Fe^{3+}] = 0.05$ M, $[Na^{+}] = 0.4$ M, $[SO_4^{2-}] = 0.35$ M), assuming that formation of crystalline iron oxides/hydroxides (e.g. goetite FeOOH) is kinetically suppressed. The lower dashed area indicates that pyrite (FeS_2) and elemental sulfur (S_8) can coexist in reducing conditions (where sulfate-reducing bacteria are active). The upper dashed area, which corresponds to the current aerobic oxidizing environment in the PEG/water solutions in the wood of the Vasa, shows that natrojarosite can form. The dashed lines enclose the water stability range ($E_H = 0$ for the standard hydrogen electrode).*

2. ESCA results. The shift of the core electron binding energy depends on the oxidation state or chemical surrounding of the absorbing atom, and gives information about the chemical state for the elements present. The intensity of the photoelectrons is proportional to the atomic concentration of each element in the surface of the sample. The photoelectrons are strongly absorbed by the sample itself, and only the surface layer ($< \sim 100$ Å) contributes to the signal. This means that surface contamination easily occurs. Furthermore, since vacuum is required to prevent air absorption of the photoelectrons, the reduced pressure will affect the concentration of elements in volatile compounds, e.g. water. Also, the amount of elemental sulfur may be affected since its vapor pressure is about $5 \cdot 10^{-6}$ mbar at 25 °C, clearly higher than the pressure in the instrument, which is below 10^{-8} mbar. Radiation damage of the sample (giving reduction of sulfate) is also possible, and small changes were observed in the spectra after long exposure.
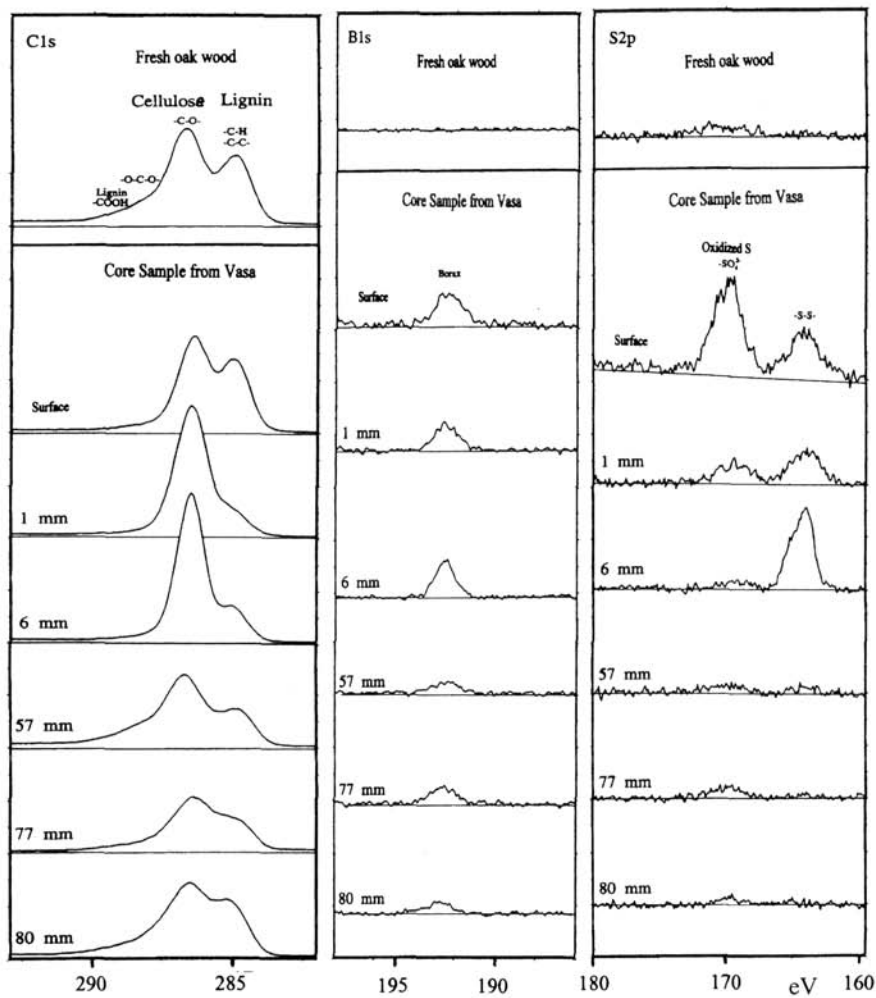
Figure 6. ESCA spectra of core C3 at various depth and fresh American red oak (top). The left figure shows the effect of different surroundings of the carbon atoms with the oxygen bonded carbon atoms (-O-C-) in PEG dominating the three top core spectra; the middle figure displays the penetration of boric acid (H_3BO_3) deep into the oak wood, and the spectra to the right show that reduced forms of sulfur are abundant in the wood below the surface.

Table 3. Results of ESCA analyses of an oak core from the Vasa and from American red oak. *Concentrations in atom%.*

Depth/mm	0	1	6	25	60	80	Red oak (bulk)
Element							
S	0.70	0.31	0.35	0.23	0.06	0.05	0.01
C	72.2	69.7	68.9	67.4	65.5	71.8	69.5
O	23.8	28.6	29.6	31.2	33.7	27.0	30.2
B	1.24	0.83	0.90	0.55	0.38	0.56	-
N	0.21	0.30	0.15	-	-	0.26	0.21
Si	0.48	-	-	-	-	-	-
Na	0.15	0.14	0.12	0.24	0.15	0.19	-
Fe	0.75	0.13	0.07	0.08	0.09	0.15	-
Cl	0.12	0.11	0.08	0.05	0.01	0.01	0.01
Ca	0.27	0.08	-	0.07	-	-	-

Sulfur: The concentration of sulfur decreases with increasing depth into the wood from a high surface value; to reach an almost constant level deep below the surface, Table 3. Note that the surface concentration is almost 20 times higher than the lowest level. Most sulfur (about 65%) on the surface was found to be oxidized to sulfate, SO_4^{2-}, while the remaining sulfur is in reduced form or embedded as elemental sulfur S_8 (*i.e.* not metal sulfide). Close below the surface the reduced forms of sulfur dominate (with about 60%) over oxidized sulfate/sulfonate (ca 40%). At 6 mm depth only about 10% of the sulfur is oxidized. At about 60 mm depth the total amount of sulfur is low, and mostly again in oxidized form. However, in another core XRD showed traces of pyrite together with elemental α-sulfur at a few mm depth.

Carbon: The outer surface is probably contaminated with C-C bonded carbon, see Figure 6. Its C(1s) spectrum is similar to that from red (American) oak but with lower -C-O- intensity. Below the surface (at 1 mm depth) the amount of -C-O- bonded carbon is appreciably higher than C-C and C-H carbon. Since the relative amount of -C-O- and –C-C- bonds in cellulose, $(C_6H_{10}O_5)_n$ (expected from standards to be C1s 83% at 286.73 eV and 17% at 288.06 eV, respectively), differs from that in lignin (phenols and alcohols), it could in principle be possible to estimate the degradation of cellulose for untreated wood. However, the polyethylene glycol, $H(OCH_2CH_2)_nOH$, only has -C-O- bonded carbon (expected C1s at 286.45 eV), and for PEG-treated wood the method could instead be used to estimate the depth of the PEG penetration. The present spectra indicate a high amount of -C-O- close to the surface, probably from PEG. At large depth the relative amount of –C-C- (lignin) carbon has increased. In fresh European oak the normal level is lignin 24.9 to 34.4 %; cellulose, 39.5 to 42.8; in sub-fossil black-oak: lignin ca 34.9 % and cellulose ca 43.2 % [9].

Boron: The initial conservation treatment of Vasa, spraying for 17 years with aqueous solutions of polyethylene glycol, also included boric acid/borax (1-4%) in the solution [3]. This is the origin of the remarkable boron concentration as oxidized borate (probably boric acid) at all depths, see Figure 6. The highest level is found at the surface, although there is substantial penetration deep into the wood.

Nitrogen is present in non-oxidized organic form, or in ammonium (NH_4^+) ions, possibly originating from the decaying organic material in the mud layer (about 5 m) that partly covered the Vasa.

Iron occurs in oxidized form with high concentration at the surface, lower below. The rusting nails, bolts and iron objects (cannon balls), which have been present, are the likely sources. However, for the lowest iron concentrations contamination when sampling (hand

operated steel drill) can possibly contribute as a source of iron for this extremely surface sensitive method, and should be checked.

Chlorine is present in small amount (0.01-0.02 atom%) deep into the wood, and also in fresh red oak. The concentration is markedly higher close to the surface, as expected from the exposure to the brackish water in Stockholm harbor.

Sodium is present in the entire core sample, but contrary to the chlorine gradient, there is no decrease deeper down into the wood. No sodium was found in the red oak sample.
Calcium was concentrated to the outermost surface layer, with a binding energy of the electrons (348.0 eV) which well corresponds to that of gypsum, $CaSO_4 \cdot 2H_2O$.

Silicon only occurs at the surface, and silicates are a typical surface contamination.

It is noteworthy that the level of manganese and potassium was too low to be detected in the analysis, and phosphorous only in trace amounts.

3. Sulfur K-edge XANES results. The position of the sulfur K-edge, i.e. the energy needed for releasing a photoelectron, is sensitive to the oxidation state [4,8]. The correlation between the oxidation state and the shift of about 13 eV from sulfides, S(-II), to sulfate $S^{VI}O_4^{2-}$, and also the shape of the absorption edge, can be used to qualitatively identify the type of sulfur compound [5,7].

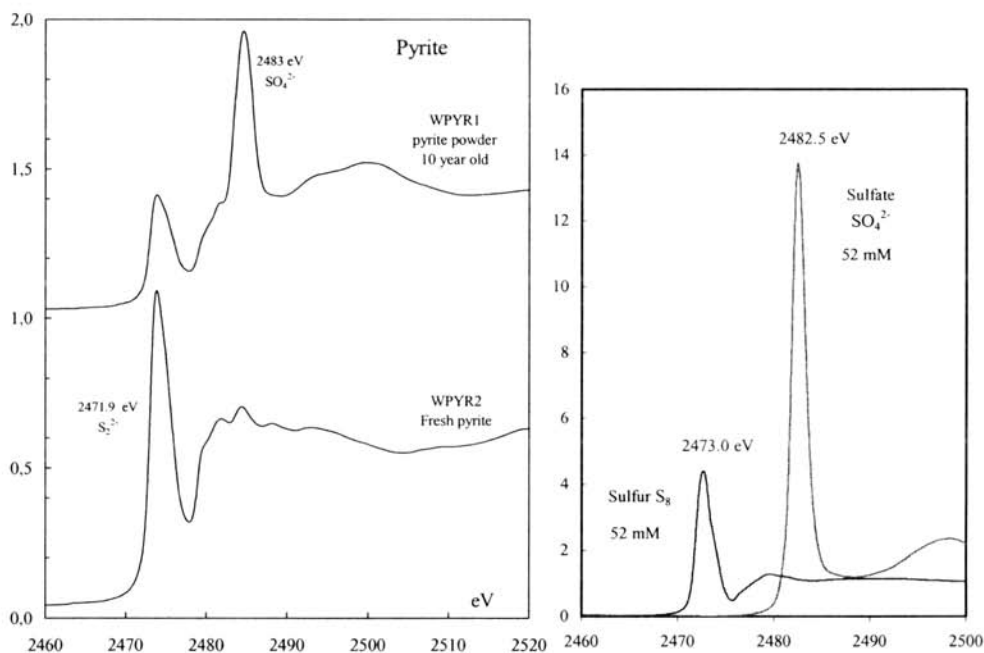*Figure 7. (left) Sulfur K-edge XANES spectra of: WPYR1: pyrite powder stored for 10 years, main part oxidized to rhomboclase $HFe(SO_4)_2 \cdot 4H_2O$ giving a major peak from the sulfate ion SO_4^{2-}, at 2483 eV; WPYR2: Freshly ground pyrite FeS_2 crystals with the main peak from the disulfide ion S_2^{2-} ion at 2471.9 eV; a minor sulfate peak at 2482.8 eV, and some intermediate oxidation states; (right) Calibration spectra of elemental sulfur in p-xylene solution and of sodium sulfate in aqueous solution. Note the intensity difference for the same sulfur concentration.*

The ESCA analyses give the concentration with fairly good accuracy of many elements, but in some cases only an estimate of the oxidation state. For sulfur, the most important element in the current study, the XANES spectra give better resolution and sensitivity. Even though the absolute concentration is difficult to determine by XANES, it is possible to classify the different types of sulfur compounds present in the samples, and also determine their relative amounts by matching the intensity with spectra from standards. The oscillations in the absorption after the edge (or after the sulfate peak) are partly caused by multiple scattering, etc., and are not treated here. Typical sulfur K-edge spectra, from pyrite, FeS_2, in fresh and oxidized state, are shown in Figure 7, and Figure 8 show the XANES spectra from the surface samples S3, S4, S7 and S8, and from the core C3 (beside S8).
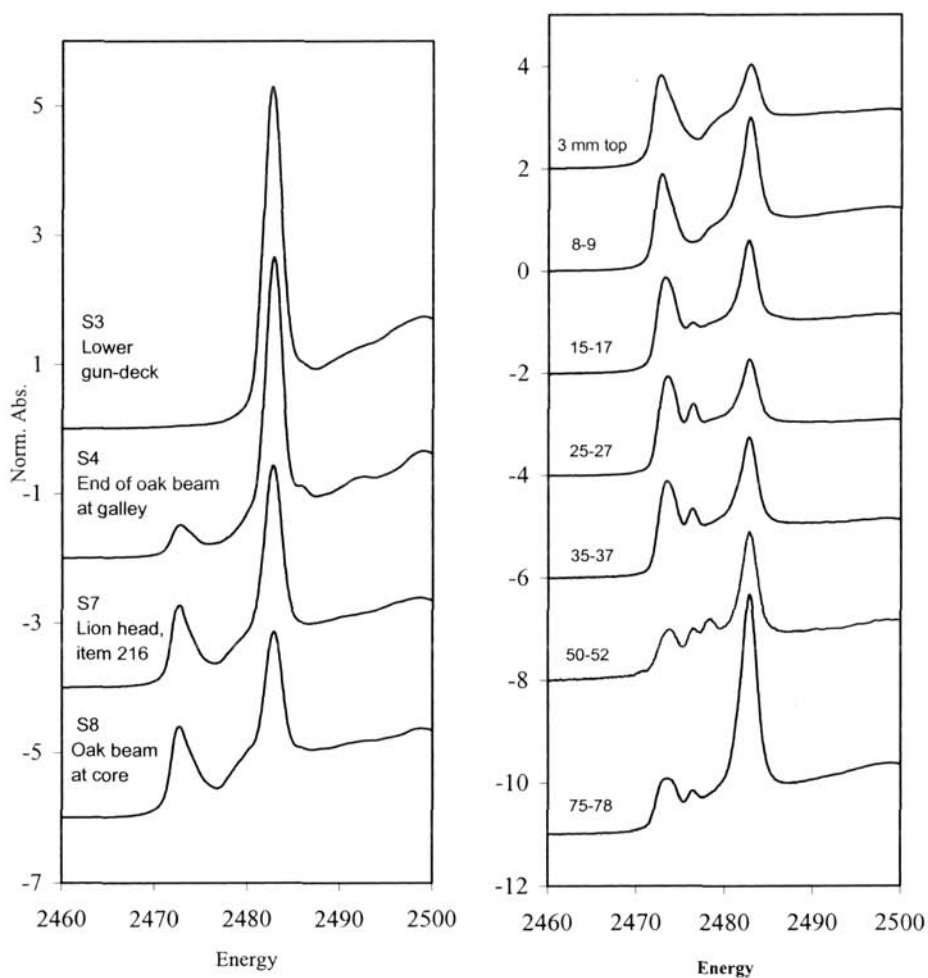

Figure 8. (left) Sulfur K-edge XANES spectra of surface samples, showing a major peak from sulfate, SO_4^{2-}, at 2483 eV and a smaller peak at 2473 eV from elemental sulfur;
(right) The spectra from the core sample C3 (at position S8) at various depths (in mm) with some intermediate oxidation states visible

79

Table 4. Results of sulfur K-edge XANES analyses of samples from the Vasa (cf. Figure 7, 8)

Description Samples from the Vasa	**Major features in sulfur K-edge spectrum** Peak energies and probable assignments	
	Major peak (eV)	minor peaks (eV)
S3 White yellow-brown crystals, Lower gun-deck at staircase	2482.6 sulfate	2481.6
S4 White cover on soft wood, at end of oak-beam Galley below lower gun-deck	2482.9 sulfate	2472.5 elem. sulfur (S_8), 2474.4, 2480.0
S7 White powder, soft (linden) wood Head of lion on gun-port, item 216 in magazine	2482.8 sulfate	2472.3, 2476.3, 2477.9, 2478.9, 2479.9, 2481.4
S8 Colorless crystals and brown-black surface layer on oak beam, close to drill holes for core samples	2483.0 sulfate 2472.3 elem. sulfur S_8	2474.6, 2476.2, 2477.9, 2479. 1, 2480.1

Core of 70 mm oak (Fig. 8):

from oak beam in hold	Major peak (eV)	minor peaks (eV)
0-1 mm from top (surface layer)	2482.6 sulfate	2472.7 elem. sulfur (S_8), 2474.6, 2476.4, 2478.2, 2481.1
1-2 mm from top	2482.7 sulfate	2472.7 elem. sulfur (S_8) 2474.4, 2478.2, 2481.2
6-7 mm from top	2472.6 elem. sulfur S_8,	2483.0 sulfate, 2476.3, 2477.9
13-14 mm from top	2472.8 elem. sulfur S_8	2482.7 sulfate
20-21 mm from top	2472.8 elem. sulfur S_8	2482.7 sulfate, 2474.0, 2476.3
65-66 mm from top	2482.7 sulfate	2473.1 elem. sulfur S_8, 2474.3, 2476.1, 2479.5, 2481.0

Calibration samples

WPYR2: Freshly ground pyrite (*Fig. 7*) crystals from mineral, powder with metallic luster	2471.9, S_2^{2-} in FeS_2	2476.1, 2477.7, 2480.0 2482.8 sulfate

WPYR1: 10-year-old pyrite powder (*Fig. 7*) Major peak at 2483 eV from sulfate ion SO_4^{2-}, (particle size < 32 μm) oxidized mainly minor peak at 2472 eV from disulfide ion S_2^{2-} to rhomboclase $HFe(SO_4)_2 \cdot 4H_2O$ (by XRD)

WPYR3: 10 year old pyrite powder (*Fig. 7*) Major peak at 2483 eV from sulfate ion SO_4^{2-}, Heated to 180 °C for 2 weeks, giving minor peak at 2472 eV from disulfide ion S_2^{2-} mainly iron(III)sulfate, $Fe_2(SO_4)_3$

Melanterite $FeSO_4 \cdot 7H_2O$ 2482.6 sulfate SO_4^{2-} 2481.5 (shoulder)

Discussion

Surface samples: The XRD analyses of the crystalline salts formed on the surfaces of the Vasa´s hull (Table 2) show different metal ions in various sites, while only two kinds of anions were found, sulfate and borate. The borate certainly originates from the initial conservation treatment with boric acid in the PEG solutions. In the sample S(taken in the hold close to the core sample, the XRD analysis also showed elemental sulfur S_8 to be present. The high concentration of sulfur in the surface of the timbers and close below, strongly indicates that sulfur, probably in the small uncharged H_2S molecule from bacterial action [6], have penetrated the wood during the 333 years in anaerobic conditions at the bottom of Stockholm harbor. The hydrogen sulfide content in the water at the place where the Vasa sank was 7 mg/L in 1943 [8]. No remaining sulfide has been found in the wood and only traces of pyrite FeS_2. The redox conditions [6] in the anaerobic environment (Figure 5), and the large amount of non-oxidized sulfur now present as elemental sulfur, S_8, show that the transition of sulfide to elemental sulfur or pyrite has taken place on the sea bottom.
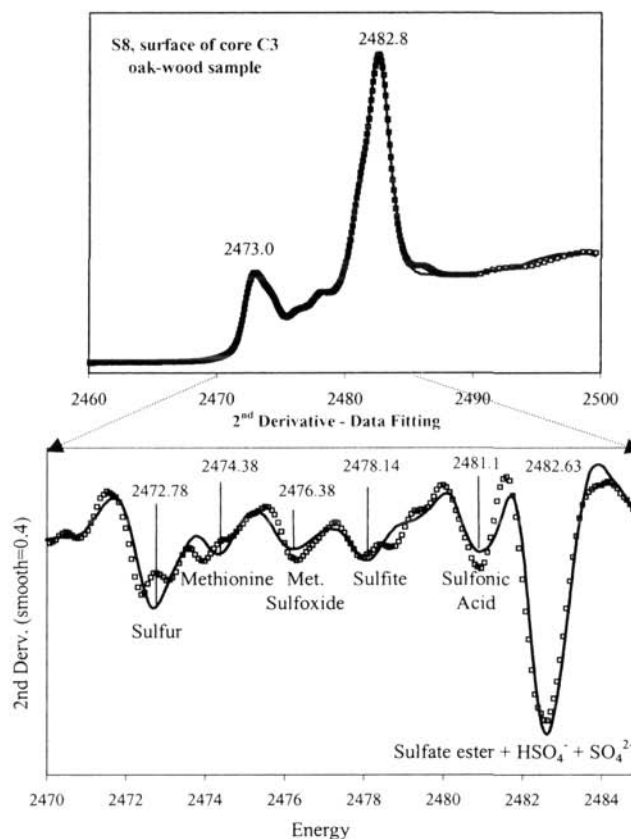

Figure 9. (top) Sulfur K-edge XANES spectrum and (bottom) 2nd derivative of surface sample S8 (dots), showing curve fitting with standards (solid lines) to analyse the relative amount and types of sulfur compounds present, from elemental sulfur at 2473 eV, to sulfate, SO_4^{2-}, at 2482.8 eV. A number of intermediate compounds are evident.

ability to penetrate into the wood. The sulfuric acid which must have formed during the 17 year spray treatment period, probably was neutralized by the borax (1-4%) dissolved together with boric acid in the PEG/water spray solution [3].

Salt formation. The variations in the relative humidity and thus the water migration in the wood, play an important role for the salt precipitation on Vasa. Water-PEG mixtures dissolve most sulfate salts readily, giving electrolyte solutions with ions in high concentration. All crystalline sulfate salts found on the hull of Vasa (Table 2) are soluble in water, except gypsum, $CaSO_4 \cdot 2H_2O$ and natrojarosite $NaFe_3(SO_4)_2(OH)_6$. Movements of water or water-PEG mixtures in the wood will therefore be able to transport salt solutions to the surface, where evaporation causes crystallisation. Decreasing the relative humidity level will cause the water content to become lower in the wood, and thereby also give less electrolyte transport, but should in the short term increase the salt precipitation.

A possible scenario for the salt precipitation in the fall of 2000 can be as follows:

- The higher humidity (> 65% RH) levels in July/August increased the amount of electrolyte solution in the surface layer of the wood, as well as the electrolyte transport.
- After September 2000, when the relative humidity level decreased back to below 60%, the decreasing water content gave a more concentrated electrolyte solution and salt precipitation.
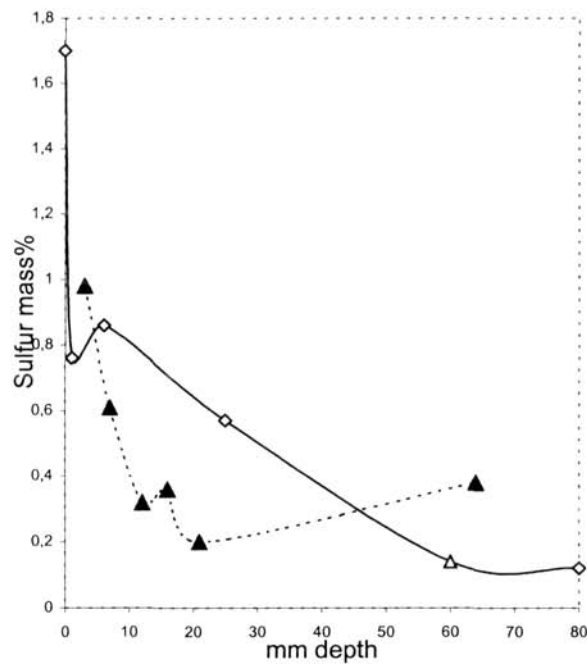

Figure 10. Total sulfur concentration in mass% S of two neighboring oak cores of 5 mm diameter at various depths by elemental analysis (filled squares) and by ESCA analysis (triangles)

83

The volume expansion is very large when sulfur compounds are oxidized to become hydrated crystalline sulfate salts, *cf.* Table 1, and may cause mechanical damage if it takes place within the wood structure. For the soluble salts found to form on the Vasa this seems not to be a major problem, because these precipitates are mostly formed on the surface when the water content decreases. Such corrosion products can be removed with a suitable treatment of the surface, see below. It has been found that if there is enough calcium present, crystallization of gypsum can take place inside the wood when sulfur is oxidized to sulfate [2], a process that certainly will damage the wood structure because of the very large volume per sulfur atom of gypsum, *cf.* Table 1. However, for the Vasa the present ESCA analysis showed calcium to be present mostly in the surface layer of the core sample. *The salt formation observed on the surfaces is, however, a sign of an ongoing production of sulfuric acid which causes high acidity, and eventually wood degradation.*

Further studies and proposed measures to be taken.
The present study has given quantitative and qualitative information on the distribution and state of the elements in the wood to an extent that has not been available before. The powerful combination of ESCA, sulfur K-edge XANES and XRD powder diffraction has revealed that there is a a large amount of reduced sulfur in the wood that currently is being oxidized, which poses a severe threat to Vasa. What measures can be taken?

Reaction rates. The main form of non-oxidized sulfur present in the Vasa is elemental sulfur, and the overall oxidation process is then

$$S(s) + {}^3/_2 O_2 + H_2O \rightarrow 2 H^+ + SO_4{}^{2-} \tag{2}$$

This reaction requires water and oxygen, O_2, probably with diffusion controlled transport dissolved in a water-PEG mixture. The following conditions can then influence the reaction rate of the reaction (2):

1. The vapor pressure of water, which is controlled by the relative humidity (RH), is directly connected to the water activity in the wood. Thus, by lowering the RH from 60% to 55% the water activity should become reduced by about 9%. This will reduce the reaction rate by about 9 % if the oxidation process is first order with respect to water, and somewhat more for higher orders. This will only cause some slowing down in the process, and the cost can be considerable for a big exhibition hall. If, however, the reaction is catalyzed by bacteria, a reduction in RH may have larger effect. A microscopic investigation for microbial activity is under way. However, the relatively low RH, and also the high borate concentration in the wood, do not favor microbial activity in the wood of the Vasa.
2. The following disadvantages may occur when lowering the humidity: *a.* The salt precipitation will increase from already saturated solution in the wood; *b.* Cracks may form in the wood, giving oxygen easier access through the PEG layer. If the oxidation process is diffusion controlled by the oxygen transport this may even increase the overall reaction rate.
3. The reaction is catalyzed by iron(III) ions, which have high concentration in some places. The higher reaction rate in such places will then influence the overall reaction rate.
4. The temperature will also affect the reaction rate. As a rule of thumb, increasing the temperature 10 degrees will approximately double the reaction rate. Thus, a fairly low and constant temperature in the exhibition hall is favorable to slow down the oxidation process.

To conclude, in order to significantly impede the reaction rate of the oxidation process the relative humidity must be lowered substantially, and this may give unacceptable side

effects. More important is to keep the conditions constant, i.e. constant relative humidity and also low temperature, in order to prevent water and oxygen migration in the wood.

Treatment of acidified wood. It is necessary and urgent to increase the pH in the acidified wood/wood surfaces. The ongoing oxidation and production of acid also requires this neutralization procedure to be made repeatedly.

- The amount of non-oxidized sulfur remaining under the surfaces, hidden and exposed, in different parts of the hull, needs to be mapped further to appreciate the extent of this problem. Core samples should be taken and analyzed from several representative spots. In particular, analyses should be made in places where the timbers already have degraded on the surface and where the acidity is high, indicating high sulfur levels, and also where high iron concentrations can be expected. Microscopic investigations should be performed to find out whether photosynthetic sulfur bacteria are, or have been, active in the wood [7,10].

- Some parts of the hull, and many items on the ship have been painted or treated differently than the bulk of the timbers, or the wood is different. For example, the ornamental lion head of linden wood, item 216 and sample S7, had corroded severely in a relatively short time in a magazine cup-board, and showed from the XRD analysis a different composition of the corrosion products, with magnesium sulfate salts, Table 2. Also, the hold of the Vasa, which has large acidified wood areas, has only been treated with PEG600, and has not got a surface treatment with PEG4000. These parts may need special treatment.

- A comparison with the Dutch East Indiaman, *Batavia*, which sank outside the Australian western coast in 1629 [1], would be of interest. An encapsulating marine concretion provided a protective anaerobic environment for a part of the hull. In this closed environment the timbers were covered by a series of iron cannon, which together with several thousands of rusting cannon balls, provided high iron concentrations. The iron corrosion products diffused into the oak wood, and probably reacted with hydrogen sulfide to form pyrite (FeS_2) and pyrrhotite (FeS) inside the wood [1,11]. This is consistent with the redox conditions as shown in Figure 5. Thus, the iron and sulfur compounds in the *Batavia's* timbers seem to have different composition and higher concentration than those in Vasa. The presence of pyrite in the Vasa's timbers is small. The chemical problems with the very high iron content and pyrite oxidation in the timbers of *Batavia* [1,11], certainly seem more severe than those for the Vasa. On the other hand, consolidation treatments, e.g. with ammonia vapor [11], or with an effective chelating agent for iron, is easier to apply for the loose timbers, which constitute the exhibition object of the *Batavia*.

- How to remove salt precipitations from degraded wood? All salts, which mechanically can be removed without affecting the wood, should be removed accordingly. Sulfate salts as $(K,NH_4)NaSO_4 \cdot 2H_2O$ (lecontite), $MgSO_4 \cdot 4H_2O$ (starkeyite) and $(NH_4)_2SO_4$ (mascagnite) can be washed away with a dilute sodium hydrogencarbonate solution in a water-PEG mixture. Compounds such as $CaSO_4 \cdot 2H_2O$ (gypsum), $FeSO_4 \cdot 4H_2O$ (rozenite), $NaFe_3(SO_4)_2(OH)_6$ (natrojarosite) and $FeSO_4 \cdot 7H_2O$ (melanterite), probably require a chelating agent dissolved in an aqueous solution of sodium hydrogencarbonate. EDTA (or rather a solution of the sodium salt of ethylenediamine tetraacetic acid) is suitable for $CaSO_4 \cdot 2H_2O$ and $MgSO_4 \cdot 4H_2O$, while for iron salts a special chelating agent is available, EDMA (the sodium salt of ethylenediiminobis(2-hydroxy-4-methyl-phenyl)acetic acid, *cf.* Figure 11), which makes iron salts soluble up to about pH 11 without precipitation of iron(III) oxide/hydroxide.

Removal of iron salts using citrate as a complexing agent (used e.g. for treatment of items from the Mary Rose and Batavia) has maximum efficiency at fairly low pH values. Calculations show that the highest solubility of iron-citrate complexes in equilibrium with

iron(III) hydroxide/oxide (goetite) occur around pH = 4, see Figure 12. It is preferable to treat especially degraded wood at a slightly alkaline pH to neutralize the acidic wooden surfaces. This is possible with EDTA (Figure 11), and in particular with the sodium salt of EDMA, which is a much stronger complexing agent [12]. The non-toxic iron(III)-EDMA complex shown in Figure 11 is used on alkaline soils as iron fertilizer. Hydrated iron(III) oxide and even hematite $Fe_2O_3(s)$ are slowly dissolved in solutions of such phenolic chelating ligands [12]. For maximum efficiency for metal removal and pH raising, treatment with a solution consisting of a mixture of the chelating agents EDTA, EDMA, buffered to about pH = 10 with a mixture of $NaHCO_3/Na_2CO_3$ can be suitable. The deep red color of the iron(III) complex with EDMA, probably requires washing with a dilute water/PEG solution of sodium hydrogen carbonate after the treatment. An application procedure should be tested out, which technically allows treatment of the wooden surfaces with such an alkaline complex-forming solution, followed by analyses after the treatment, to evaluate the effect and usefulness of the method.
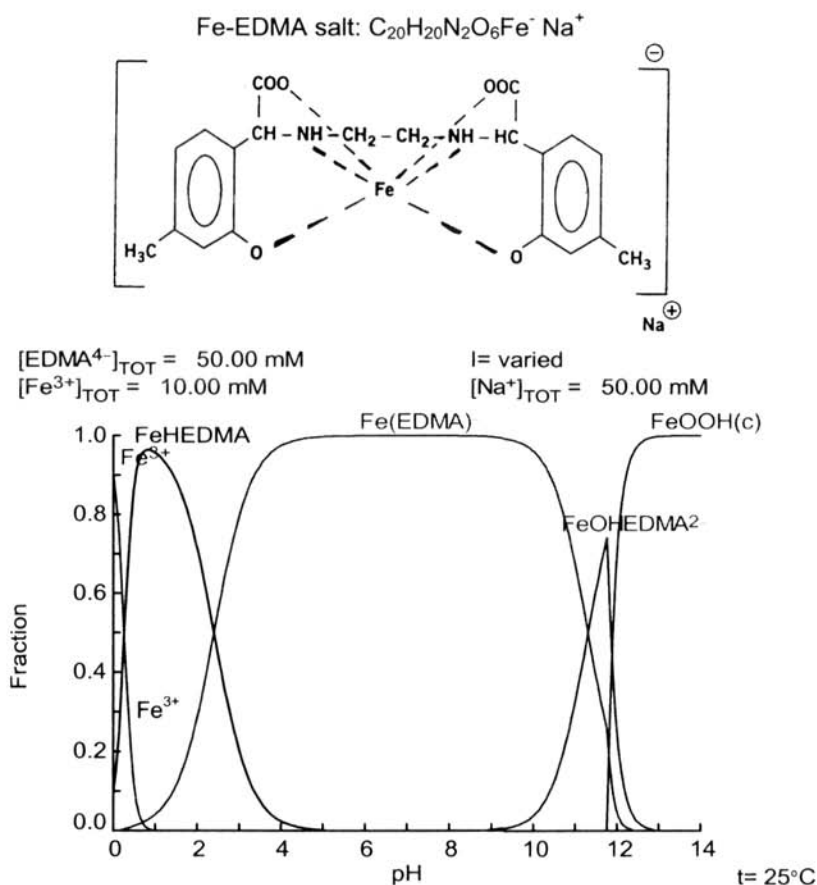

Figure 11. The deep red iron(III) complex [Fe(EDMA)]⁻ formed with the chelating EDMA⁴⁻ anion is capable of keeping iron(III) ions in solution and dissolving crystalline goetite FeOOH(c) up to pH 11. Equilibrium constants from Ref. [12].
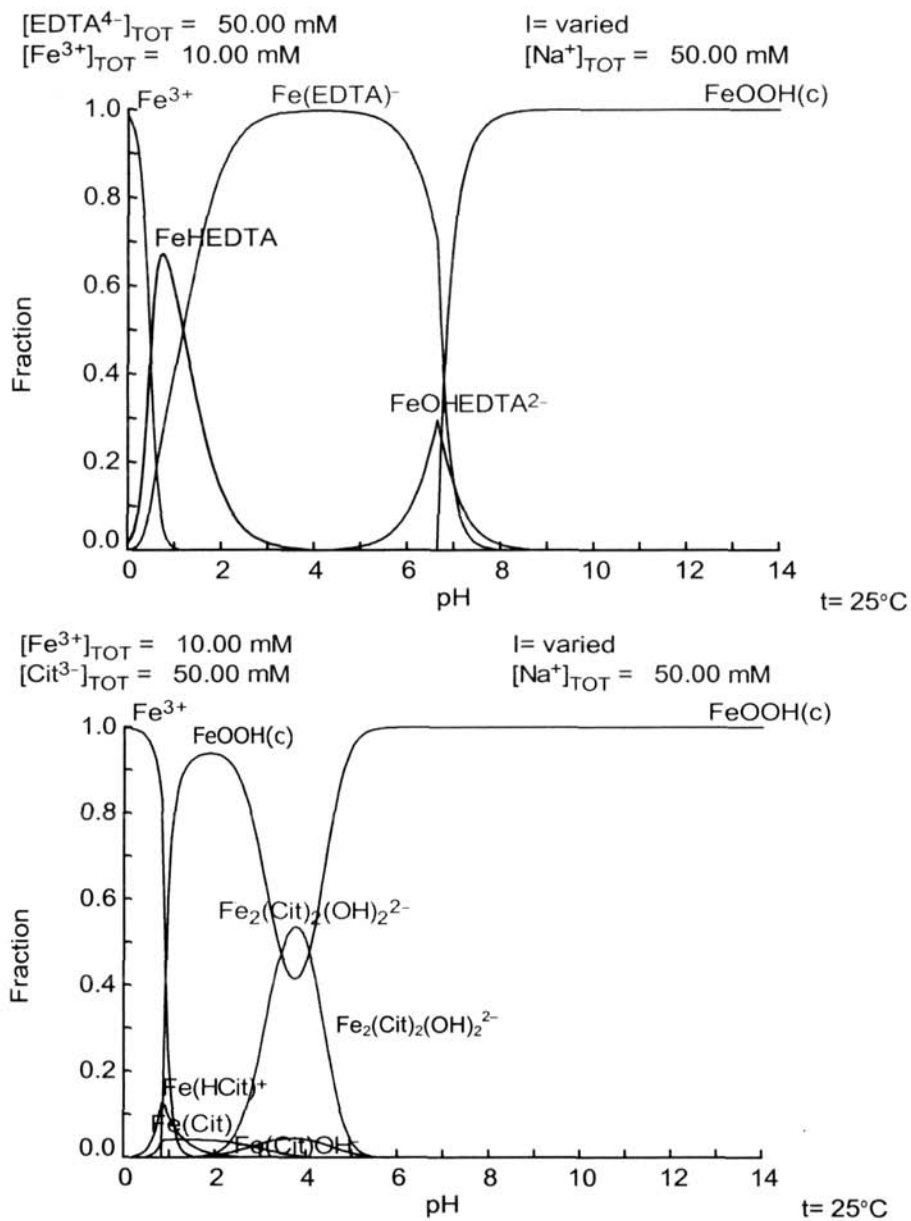
Figure 12. pH diagrams showing the solubility of iron(III) in the form of crystalline goetite, FeOOH(c), in EDTA (top) and in citrate (lower) solutions. Equilibrium constants are those from the database HYDRA connected to the MEDUSA program [13], complemented by Ref. 12 for the EDTA complexes.

- Another aspect is the degradation of PEG. In a recent thesis the biological degradation of waterlogged archaeological wood has been shown to be caused by bacterial action ("erosion" bacteria), in low-oxygen environment [10]. A water-filled skeleton of cell walls then remains, for which the water has to be replaced by a filling material, *e.g.* PEG to keep the structure intact without cracking. It is now known that metallic iron rapidly corrodes in contact with PEG [14], indicating that there is a specific metal surface-PEG interaction and/or complex formation between PEG and iron ions.
- It is possible that the transition metal ion pair iron(II)/iron(III) catalytically can oxidize PEG in solution. This can be followed by NMR methods. Structural information on the preferential complexation and interactions of the metal ion pair iron(II)/iron(III) with PEG in solutions of different concentration and composition is essential for understanding such a process. Because PEG is a non-crystalline polymer and the metal concentration is relatively low, the synchrotron based XAS method, now analyzing the extended X-ray absorption fine structure (EXAFS) of the iron K-edge, is the only technique, which will give useful structural information. Also, catalytic degradation of cellulose with iron ions has been proposed.
- More than 8000 iron bolts, mostly zinc or epoxy-coated and up to 1.5 m long, were used to replace the corroded original bolts of Vasa, to hold the hull together (Figure 13). Many of these "new" bolts show severe corrosion in the PEG-treated wood and should be replaced As an aid to choose a suitable corrosion-resistant material for new bolts, e.g. acid resistant stainless steel or titanium, the PEG-metal surface interaction should first be studied by ESCA.

Figure 13. Oak beams at upper gundeck inside the Vasa, showing some corroding iron bolts. The white lines are from surplus PEG4000 from the surface treatment.

VASA

References

1. MacLeod, I.D. and Kenna, C., *Degradation of archaeological timbers by pyrite: Oxidation of iron and sulphur species*, in Proceedings of the 4th ICOM Working Group on Wet Organic Archaeological Materials Conference, Bremerhaven, 20-24 August 1990, ed. P. Hoffmann, ICOM, Committee for Conservation Working Group on Wet Organic Archaeological Materials, Bremerhaven, pp. 133-142.
2. Jespersen, K. (1989). *Precipitation of iron corrosion products on PEG-treated wood*. In Conservation of Wet Wood and Metal, Proceedings of the ICOM Conservation Working Groups on Wet Organic Archaeological Materials and Metals, Fremantle 1987, pp. 141-152. Western Australian Museum.
3. Håfors, B. in *Archaeological Wood, Properties, Chemistry and Preservation* (eds Rowell, R. M. & Barbour, R. J.) 195-216 (Advances in Chemistry Series 225, American Chemical Society, Washington DC, 1990).
4. Gelius, U.; Wannberg, B.; Baltzer, P.; Fellner-Feldegg, H.; Carlsson, G.; Johansson, C.-G.; Larsson, J.; Münger, P.; Vegerfors, G. *J. Electr. Spectr. Rel. Phenom.* 1990, *52*, 747-785.
5. Hedman, B.; Frank, P.; Penner-Hahn, J. E.; Roe, A. L.; Hodgson, K.O.; Carlson, R.M.K.; Brown, G.; Cerino, J.; Hettel, R.; Troxel, T.; Winick, H.; Yang, J. *Nucl. Instr. and Meth.* 1986, *A246*, 797-800.
6. Stumm, W.; Morgan, J.J. *Aquatic Chemistry, Chemical equilibria and Rates in Natural Waters*, Wiley-Interscience, New York 1996, 3rd ed., Chapter 8.5.
7. Pickering, I. J.; George, G.N.; Yu, E.Y.; Brune, D.C.; Tuschak, C.; Overmann, J.; Beatty, J.T.; Prince, R.C. *Biochemistry*, 2001, *40*, 8138-8145.
8. Barkman, L. *Conservation of rusty iron objects by hydrogen reduction*, National Bureau of Standards, Special publication 479. Issued July 1977.
9. Wagenführ, R.; Scheiber, C. *Holzatlas*, VEB Fachbuchverlag Leipzig, 1985, 2nd ed., pp. 432- 437.
10. Björdahl, C. *Waterlogged Archaeological Wood, Biodegradation and its implications for conservation*, Thesis, Swedish University of Agricultural Sciences, Uppsala, 2000.
11. Richards, V.L., *The consolidation of degraded, deacidified Batavia timbers*, Australian Institute for the Conservation of Cultural Material, *Bulletin* 1990, *16*, 35-53.
12. Ahrland, S., Dahlgren, Å. and Persson, I. *Acta Agric. Scand.* 1990, *40*, 101-111.
13. Puigdomenech, I. Computer program MEDUSA and data base HYDRA with equilibrium constants at 25 °C, available at: http://www.inorg.kth.se/Medusa/.
14. Guilminot, E.; Dalard, F.; Degrigny, C. *Eur. Fed. Corros. Publ.* 2000, *28*, 300-309.

89